Supplementary Information

Biomass-based N, P, S Self-doped Porous Carbon for High

Performance Supercapacitors

Guangzhen Zhao [a,b], Yanjiang Li [b], Guang Zhu [c], Junyou Shi [a,d]* Ting Lu [b,e] * and Likun Pan [b]

[a] Energy Resources and Power Engineering College, Northeast Electric Power University, 169 Changchun Road, Jilin 132012, PR China

[b] Shanghai Key Laboratory of Magnetic Resonance, School of Physics and Materials Science, East China Normal University, 3663 N. Zhongshan Road, Shanghai 200062, PR China

[c] Anhui Key Laboratory of Spin Electron and Nanomaterials (Cultivating Base), Suzhou University, Educational Park, SuZhou 234000, PR China

[d] Forestry College, Beihua University, 3999 Binjiang east Road, Jilin 132013, PR China

[e] Department of Chemical Engineering, School of Environmental and Chemical Engineering, Shanghai University, 99 Shangda Road, Shanghai 200444, PR China

*Corresponding author. Tel.: +8621 62234322

E-mail address: bhsjy64@163.com (Junyou Shi);

tlu@phy.ecnu.edu.cn (Ting Lu).

Material characterization

The surface microstructures and morphologies of samples were measured using transmission electron microscopy (TEM, Tecnai G2 F20) and scanning electron microscopy (SEM, QUANTA250). The X-ray diffraction (XRD, Rigaku D/MAX-2500 system) and Raman spectroscopy (LabRAM HR800) were used to characterize the crystallinity of all samples. X-ray photoelectron spectroscopy (XPS, Thermo Scientific ESCALab 250Xi system) was used to characterize elemental composition and chemical state. N_2 adsorption-desorption isotherm was measured by ASAP 2020 System (Micrometitics). The pore size distribution, total pore volume and specific surface area were analyzed by N_2 adsorption-desorption isotherms.

Electrochemial measurements

In a three-electrode system, the electrochemical performances of PMC, AC and N-P-S-HPC were measured by electrochemical workstation (CHI660E, CHI Instruments Co.). The obtained slurry of electrode materials was fabricated by mixing the obtained sample (80%), polyvinylidene fluoride (PVDF, 10%) and acetylene black (10%) using a certain amount of N-methyl-2-pyrrolidone (NMP) as solvent, which was cast on a carbon paper (20 × 20 mm^2) and dried (80 ˚C for 12 h) as working electrode. Ag/AgCl electrode and a Pt foil electrode (20 × 20 mm^2) were used as reference and counter electrode, respectively. The electrochemical impedance spectroscopy in the frequency range of 0.01-100000 Hz (EIS, at an open circuit potential with amplitude of 5 mV), cyclic voltammetry (CV, 2-100 mV s^{-1}), and galvanostatic charge-discharge (GCD, 1-20 A g^{-1}) were measured using a 1 M H_2SO_4 aqueous solution. The specific capacitances (C_g, F g^{-1}) of all samples were obtained from the GCD curves as follows:

$$C_g = \frac{I_d \times \Delta t}{m \times \Delta V} \qquad (1)$$

where ΔV (V) is the applied voltage window, I_d (A) is the discharge current, Δt (s) is discharge time and m (g) is the mass of active materials.

The symmetrical SC was assembled by two N-P-S-HPC electrodes and measured using a two electrode system. CV, GCD and cycle life measurements were tested in 1 M Na_2SO_4 aqueous solution. The specific capacitance (C_g, F g^{-1}), energy density (E, Wh kg^{-1}) and power density (P, W kg^{-1}) of symmetrical SC can be calculated by the GCD curves as following equations:

$$E = \frac{1}{7.2} \times C_g \times \Delta V^2 \qquad (2)$$

$$P = 3600 \times \frac{E}{\Delta t} \qquad (3)$$

Trasatti method

The Trasatti method was used to differentiate the capacitance contribution from electrical double layer and pseudo-capacitive reactions. The total capacitance (C_{Total}) and the electrical double layer capacitance (C_{EDLC}) can be estimated from the ordinate intercept by extrapolating the plot of $1/C$ vs. $v^{0.5}$ and C vs. $v^{-0.5}$, respectively, according to the following equations [1-3]:

$$C^{-1} = constant\ v^{0.5} + C_{Total}^{-1} \qquad (4)$$

where C (F g^{-1}) is experimental gravimetric capacitance, v (V s^{-1}) is scan rate and C_{Total} (F g^{-1}) is total capacitance;

$$C = constant\ v^{-0.5} + C_{EDLC} \qquad (5)$$

where C_{EDLC} is electrical double capacitance. The maximum pseudocapacitance (C_{PC}) as obtained by follow equation:

$$C_{PC} = C_T - C_{EDLC} \tag{6}$$

Dunn Method

The Dunn method can also be used to analyze the capacitance contributions from surface capacitive effects (regarded as EDLC, k_1v) and diffusion-controlled processes capacitive effects (regarded as PC, $k_2v^{0.5}$) according to the following equation [4]:

$$I(V) = k_1 v + k_2 v^{0.5} \tag{7}$$

where $k_1 v$ is contributed from EDLC effects while the term $k_2 v^{0.5}$ is associated with PC reactions.

$$I(V)/v^{0.5} = k_1 v^{0.5} + k_2 \tag{8}$$

The k_1 and k_2 values can be calculated via plotting the fitting lines of $i(V)/v^{1/2}$ and $v^{1/2}$, and then the capacitive current $i_c(V) = k_1v$ could be distinguished from the total measured current. For example, the comparison of capacitive current with the tested current from CV curves can be calculated, as shown in Figure S3. The result shows that the capacitance contributions of N-P-S-HPC from EDLC and PC value are 73% and 27% at the sweep rate of 5 mV s^{-1}.
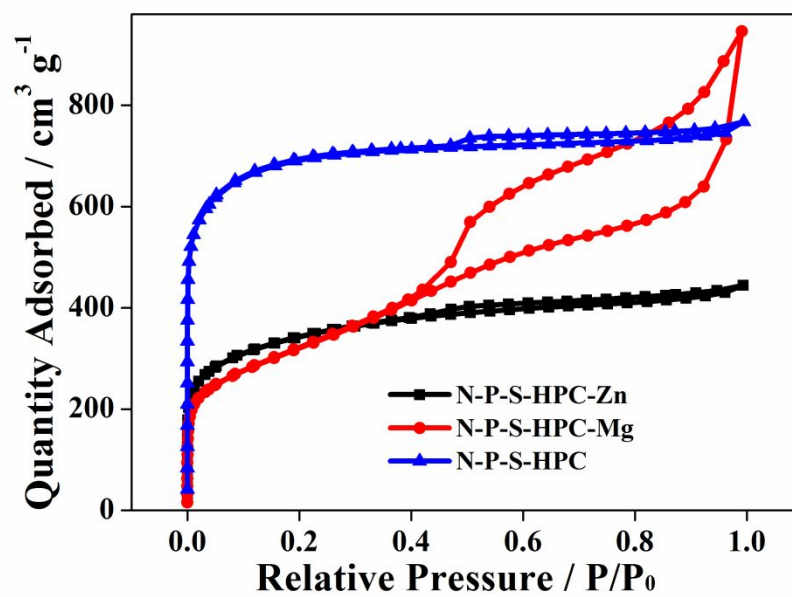
Figure S1 N$_2$ adsorption-desorption isotherms of N-P-S-HPC-Zn, N-P-S-HPC-Mg and N-P-S-HPC.
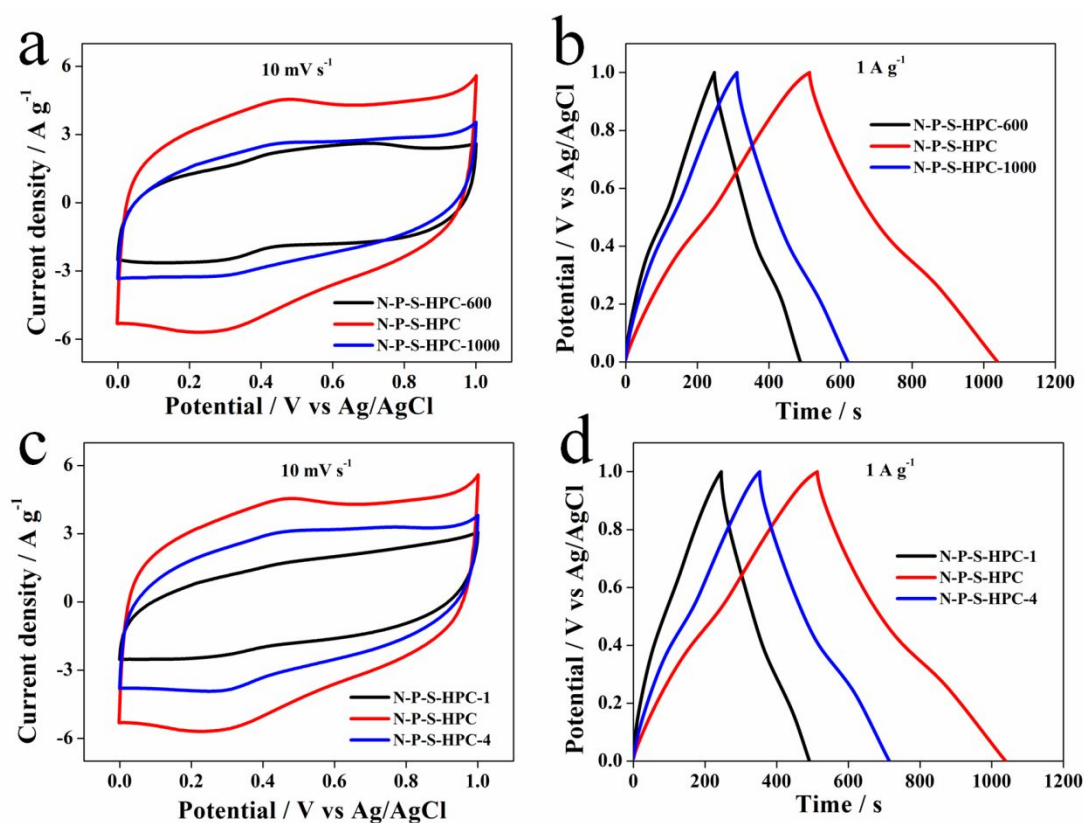
Figure S2 In a three-electrode system, electrochemical performances of all samples were tested in 1 M H_2SO_4. CV curves at 10 mV s^{-1} (a) and GCD curves at of 1 A g^{-1} (b) of N-P-S-HPC-600, N-P-S-HPC and N-P-S-HPC-1000. CV curves at 10 mV s^{-1} (c) and GCD curves at of 1 A g^{-1} (d) of N-P-S-HPC-1, N-P-S-HPC and N-P-S-HPC-4.
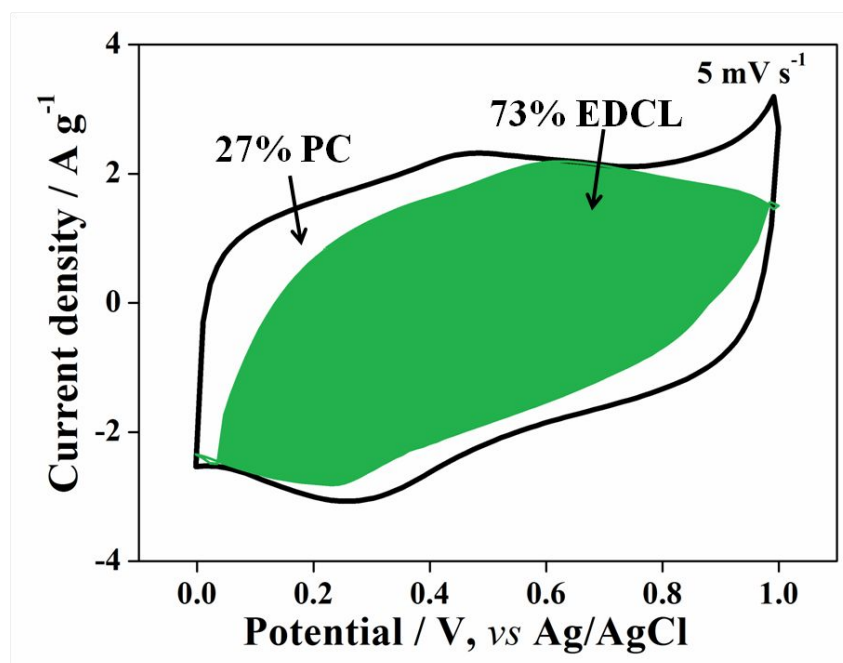
Figure S3 According to Dunn method analysis of respective capacitance contribution of N-P-S-HPC at scan rate of 5 mV s^{-1}. The yellow region outlined the current contributed from EDLC capacitance.

Table S1 The specific surface area (S_{BET}), total pore volumes (V_{total}) of N-P-S-HPC-Zn, N-P-S-HPC-Mg and N-P-S-HPC.

	S_{BET} ($m^2\ g^{-1}$)	V_{total} ($cm^3\ g^{-1}$)
N-P-S-HPC-Zn	1098	0.68
N-P-S-HPC-Mg	1264	1.21
N-P-S-HPC	2090	1.42

Reference

[1] Ardizzone G.F.S.; Trasatti S. "Inner" and "Outer" Active Surface of RuO_2 Electrodes, *Electrochim. Acta.* 1990, 35, 263-267, DOI: 10.1016/0013-4686(90)85068-X

[2] Duay J.; Sherrill S.A.; Gui Z.; Gillette E.; Lee S.B. Self-limiting Electrodeposition of Hierarchical MnO_2 and $M(OH)_2/MnO_2$ Nanofibril/Nanowires: Mechanism and Supercapacitor Properties, *Acs Nano.* 2013, 7(2), 1200-1214, DOI: 10.1021/nn3056077

[3] Lee Y.H.; Chang K.H.; Hu C.C. Differentiate the Pseudocapacitance and Double-layer Capacitance Contributions for Nitrogen-doped Reduced Graphene Oxide in Acidic and Alkaline Electrolytes, *J. Power Sources.* 2013, 227, 300-308, DOI: 10.1016/j.jpowsour.2012.11.026.

[4] Wang J.; Polleux J.; Lim J.; Dunn B. Pseudocapacitive Contributions to Electrochemical Energy Storage in TiO_2 (Anatase) Nanoparticles, *J. Phys. Chem. C.* 2007, 111(40), 14925-14931, DOI: 10.1021/jp074464w.